MATERIALES DE CONSTRUCCIÓN
Vol. 68, Issue 329, January–March 2018, e150
ISSN-L: 0465-2746
https://doi.org/10.3989/mc.2018.10716

Combined effect of nano-SiO_2 and nano-Fe_2O_3 on compressive strength, flexural strength, porosity and electrical resistivity in cement mortars

M. A. Sanjuán, C. Argiz, J. C. Gálvez✉, E. Reyes

Departamento de Ingeniería Civil: Construcción, E.T.S de Ingenieros de Caminos, Canales y Puertos, Universidad Politécnica de Madrid. C / Profesor Aranguren, s/n, 28040, Madrid. Spain.
✉jaime.galvez@upm.es

Received 16 September 2016
Accepted 17 July 2017
Available on line 6 March 2018

ABSTRACT: The compressive strength, flexural strength, porosity and electrical resistivity properties of cement mortars with nano-Fe_2O_3 and nano-SiO_2 are studied. Amorphous silica is the main component of pozzolanic materials due to its reaction with calcium hydroxide formed from calcium silicate (C_3S and C_2S) hydration. The pozzolanic reaction rate is not only proportional to the amount of amorphous silica but also to the surface area available for reaction. Subsequently, fine nano-Fe_2O_3 and nano-SiO_2 particles in mortars are expected to improve mortar performance. The experimental results showed that the compressive strength of mortars with nano-Fe_2O_3 and nano-SiO_2 particles were lower than those obtained with the reference mortar at seven and 28 days. It was shown that the nano-particles were not able to enhance mechanical strength on every occasion. The continuous microstructural progress monitored by mercury intrusion porosimetry (MIP) measurements, pore-size distribution (PSD), total porosity and critical pore diameter also confirmed such results.

Keywords: Active addition; Mortar; Compressive strength; Mechanical properties; Hydration.

Citation/Citar como: Sanjuán, M.A.; Argiz, C.; Gálvez, J.C.; Reyes, E. (2018) Combined effect of nano-SiO_2 and nano-Fe_2O_3 on compressive strength, flexural strength, porosity and electrical resistivity in cement mortars. Mater. Construcc. 69 [329], e150 https://doi.org/10.3989/mc.2018.10716

RESUMEN: *Influencia de la combinación de nano-SiO_2 y nano-Fe_2O_3 en la resistencia a compresión, resistencia a tracción, porosidad y resistividad eléctrica de morteros de cemento.* Se estudia la resistencia a compresión y flexión, porosidad y resistividad eléctrica de morteros de cemento con nano-Fe_2O_3 y nano-SiO_2. La sílice amorfa reacciona con el hidróxido de calcio formado en la hidratación del C_3S y C_2S. La tasa de reacción puzolánica es proporcional a la cantidad de sílice amorfa y la superficie disponible para la reacción, esperando que las partículas finas de nano-Fe_2O_3 y nano-SiO_2 mejoren las propiedades de los morteros. Los resultados experimentales han mostrado que la resistencia a compresión a siete y 28 días de morteros con partículas de nano-Fe_2O_3 y nano-SiO_2 era, en ocasiones, inferior a la obtenida con el mortero de referencia. Se muestra que las nano-partículas no siempre son capaces de mejorar la resistencia de los morteros. Las medidas mediante porosimetría de intrusión de mercurio (PIM) de la distribución de tamaño de poro (DTP), porosidad total y diámetro de poro crítico confirmaron estos resultados.

Palabras clave: Adición activa; Mortero; Resistencia a la compresión; Propiedades mecánicas; Hidratación

ORCID ID: M.A. Sanjuan (https://orcid.org/0000-0001-6694-0634); C. Argiz (https://orcid.org/0000-0003-4519-872X); J.C. Gálvez (https://orcid.org/0000-0001-9106-2917); E. Reyes (https://orcid.org/0000-0002-1284-7335)

1. INTRODUCTION

The larger specific surface of new pozzolanic materials (1, 2) leads to a higher degree of reactivity (3). In addition, new ultra-high strength concretes have been designed by using fine silica fume and being based on a densified system that contains homogeneously arranged ultra-fine particles. They have been named reactive powder concretes (RPCs) (4). Therefore, fine silica fume performs better than a coarse one in terms of mechanical strength (5). A nano-SiO_2 addition is then expected to enhance compressive strength with regard to silica fume (6).

Nano-SiO_2 in cement-based materials usually improves mechanical strength (7-16), lowers and refines porosity (17), shortens the C_3S hydration acceleration period, and enhances C-S-H gel precipitation and nucleation (18, 19, 20). However, another key factor that influences nano-SiO_2 reactivity is the densification state (21, 22). According to Haruehansapong et al (7), a nano-SiO_2 particle size of 40 nm gives higher compressive strength compared with mortars with nano-SiO_2 particle sizes of 12 and 20 nm, with it arguably being due to an agglomeration of small particles. This suggests that the resulting agglomerates will have a stronger influence on the pozzolanic, filling, and cement hydration seeding effects, all of which lead to a microstructure improvement (22).

Nano-oxides with a smaller grain size than silica fume are studied in construction products due to the new potential properties expected. This means that they can provide potential new applications when nano scale-size particles are added to cement-based materials. Thus, this provides a new manner to design alternative cement-based materials with improved properties in comparison with conventional grain-size ones. Relatively little published research deals with the combination of nano-Fe_2O_3 and nano-SiO_2 in cementitious building materials (8). All such articles have reported a significant increase in mechanical strength and porosity refining.

This paper examines the possible influence of a dispersion and curing procedure as a key factor in designing these new products based on nano-SiO_2 and nano-Fe_2O_3. Since pozzolanic and filling effects are affected by nano-oxide content, variations with nano-SiO_2 and nano-Fe_2O_3 (from 2.35% to 6% and from 2% to 4%, respectively) were also analysed. In essence, the paper studies the influence of the combination of nano-Fe_2O_3 and nano-SiO_2 on cement mortars prepared and cured in common conditions frequently found in practice.

2. EXPERIMENTAL PROGRAMME

2.1. Materials

The standard mortar composition involves use of the sulphate-resistant Portland cement CEM I 42.5R-SR 3 as a binder, a siliceous (more than 98% SiO_2) standard CEN sand according to the European Standard EN 196-1:2016 (NORMASAND) (23) and two types of nanomaterials as additions. The chemical and physical properties of the cement are presented in Table 1. A commercial nano-SiO_2 Levasil 200/40%, distributed by Obermeier and a commercial Iron III oxide nano-particles (nano-Fe_2O_3) supplied by Tecnología Navarra de Nanoproductos S.L. (TECNAN) were used (Table 2). Tap water from Canal de Isabel II (located in Madrid) was used to prepare the mortars. A modified polycarboxylate-based superplasticizer or high-range water-reducing additive (HRWRA) according to EN 934-2 (24), Sika ViscoCrete®-5720 (pH = 4; density = 1.09 kg/l and 36% solid content) was employed with a relatively low dosage of 0.15–0.3% per cement weight (Table 2). Due to its chemical structure, it enabled good particle dispersion to be obtained.

Table 1 Chemical composition and physical properties of the cement

Chemical composition	(%)	Physical properties of cement	
SiO_2	19.30	Specific gravity (kg/m^3)	3.10
Al_2O_3	3.42	Initial setting time (min)	173
Fe_2O_3	4.13	Final setting time (min)	252
CaO	67.26	Volume expansion (mm)	0.68
MgO	1.04	Specific surface area (SSA), Blaine (m^2/kg)	4116
SO_3	2.91	25 µm residue (%)	35.8
K_2O	0.32	32 µm residue (%)	24.5
Na_2O	0.16	63 µm residue (%)	3.1
P_2O_5	0.10	Hydration heat (J/g)	325
LOI	3.70	Compressive strength	(MPa)
Soluble residue[a]	0.49	2 days	30.1
Cl^-	0.019	28 days	61.0

[a] Na_2CO_3 method.

Table 2 Technical data of the commercial nano-Fe_2O_3, nano-SiO_2 and high-range water-reducing admixture

Commercial product	Nano-SiO_2	Nano-Fe_2O_3	High-range water-reducing admixture - SIKA Viscocrete 5720
Purity (%)	40.54	99.721	40.54
Density (g/cm^3)	1.295	-	1.090
pH (20ºC)	10.3	-	4
Superficial area (m^2/g)	205	60-120	-
Viscosity (m•Pa•s)	9.21	-	-

The particle size of the commercial nano-SiO_2 Levasil was 10-20 nm (this value was supplied by the producer). The specific surface area of the commercial Iron III oxide nano-particles (nano-Fe_2O_3) was 55.9 m^2/g, and the mean particle size 1.95 µm, with both being experimentally measured.

2.2. Mix design

Prior to testing the mortars, the mix design shown in Table 3 was selected in order to maximise the information recorded regarding the combined use of nano-Fe_2O_3, nano-SiO_2 in mortars.

All the mortar mixes had the same water/cement ratio of 0.5. The water provided by the Nano-SiO_2 solution was deducted from the mixing water of the mortar. In addition, a high-range water-reducing admixture (HRWRA) was adopted in order to obtain similar slump in all mixes.

2.3. Flexural and compressive strength testing

Flexural and compressive strength tests were performed in 40x40x160mm mortars at two, seven and 28 days according to the European Standard EN 196-1: 2016 (23). The specimens were cured at 95% relative humidity in a humidity-testing cabinet at 20.0±1.0ºC.

The curing process of the specimens was carried out according to the European Standard EN 196-1:2016. This standard method allows results to be compared under the same curing conditions for all the specimens. In accordance with Sajedi and Razak, (29) the compressive strength of the mortar is highly dependent on the curing conditions.

Flexural strength was measured on three specimens for each mortar mix. The six samples obtained after the flexural strength testing were used for compressive strength testing. Flexural strength values were calculated according to the following equation [1].

$$R_f = \frac{1{,}5 * F_f * l}{b^3} \qquad [1]$$

where R_f is flexural strength (MPa), F_f is load applied in the middle of the specimen (N), l is side of the prism (mm) and b is distance between the two steel supporting rollers (mm).

2.4. Mercury intrusion porosimetry (MIP)

A mortar porous system (with total open porosity and pore-size distribution) was studied at 28 days by means of mercury intrusion porosimetry (MIP) in "Phi mayúscula"12x40 mm cylindrical samples, in a range of pore radius between 0.005 and 180 µm following an internal procedure based on the ASTM D4404-04. The samples were oven-dried at 40±5°C for four days and then analysed with use of a Micromeritics AutoPore IV 9599 porosimeter.

The porosity of a material affects its physical properties and, subsequently, the mechanical strength and durability performance. In particular, the total porosity and pore-size distribution (PSD) give information regarding the open porosity. Therefore, it could serve as an indirect indicator of the permeability of the sample in certain cases. In essence, porosity measurement is a suitable tool in enabling an understanding of microstructure evolution and potential use of nano-oxide-made mortars.

By measuring the volume of mercury that intrudes into the sample material with each pressure change, the volume of pores in the corresponding size interval is obtained. Then, the total porosity can be calculated according to equation [2].

$$P_t = \frac{V_p}{V_m} * 100 \qquad [2]$$

where P_t is the total porosity (%), V_p is the porous volume (mm^3) and V_m is the sample volume (mm^3).

2.5. Resistivity

Resistivity is a non-destructive test method described extensively in the Spanish Standard UNE

Table 3 Mortar mixes

Mix code	M0	M3.5Si2Fe	M2.35Si4Fe	M6Si2Fe	M4Si4Fe
Nano-SiO_2 (%)(*)	0	3.5	2.35	6	4
Nano-Fe_2O_3 (%)(*)	0	2	4	2	4
Sand(g)	1350	1350	1350	1350	1350
Water (g)	225	202.0	209.5	185.5	198.7
Cement (g)	450	450	450	450	450
Nano-Fe_2O_3 (g)	0	9	18	9	18
Nano-SiO_2 (g)	0	38.8	26.0	66.5	44.3
High-range water-reducing admixture (g)	0	1	0	2	1

(*) % weight of cement

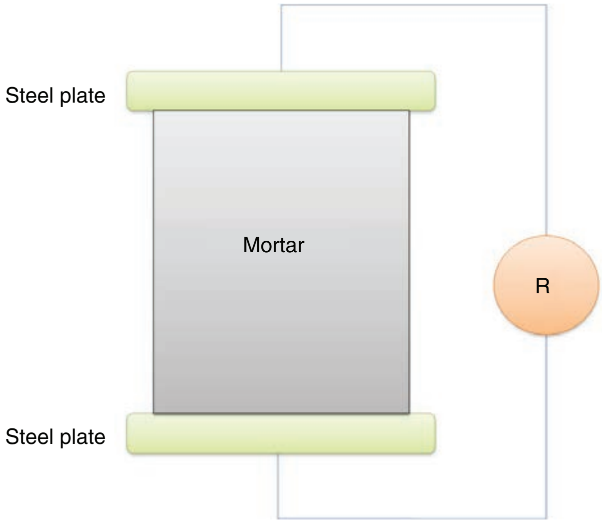

FIGURE 1. Two-electrode testing on mortar prism.

83988-1 (26). The test was performed on 40 x 40 x 160 mm mortar prisms at 60 days for M6Si2Fe and M4Si4Fe specimens and at 90 days for M2.35Si4Fe y M3.5Si2Fe specimens. Electrical resistivity was determined by use of the two-electrode method (Giatec RCON™) that measures electrical resistance with frequencies between 1 Hz and 30 KHz (Figure 1). Equation [3] was used to calculate electrical resistivity.

$$R = \frac{V}{I} = \rho \frac{l}{A} \quad [3]$$

where R is electrical resistance, ρ is electrical resistivity, V is potential difference, I is current intensity, l is steel plate distance and A is area (Figure 1).

Electrical resistivity measurements give information about the open porosity of the mortar and concrete. The Nernst-Einstein equation expresses the relationship between the electrical resistivity and ion diffusivity for porous materials (27). Therefore, it is possible to estimate the diffusivity of the mortar and concrete by measuring resistivity, as shown in equation [4].

$$D_i = \frac{1}{\rho} * k \quad [4]$$

where D_i is diffusivity for ion i, ρ is electrical resistivity and k is a constant value obtained from the slope of the linear correlation between the ion diffusivity and electrical conductivity, which is the inverse parameter of the electrical resistivity (Table 4).

A clear relationship between corrosion rate and electrical resistivity can be found in most of the cement-based materials (28).

TABLE 4 Relationship between electrical resistivity and ion diffusivity according to ASTM C1202 (25) and UNE 83988-1 (26)

Chloride diffusivity	Charge (Coulomb) ASTM C1202	Electrical resistivity (Ω·m) UNE 83988-1
High	4000	<50
Moderate	2000 a 4000	50 a 100
Low	1000 a 2000	100 a 200
Very low	100 a 1000	200 a 2000
Insignificant	< 100	>2000

3. RESULTS AND DISCUSSION

3.1. Flexure strength and compressive strength

The results obtained for flexure and compressive strength at two, seven and 28 days, and their standard deviation in MPa, are shown in Figure 2 and Figure 3, respectively.

All the mortars made with nano-oxides showed compressive strength results below the reference mortar made without additions. These results differ from others reported elsewhere (7-16). Usually, nano-Fe_2O_3 and nano-SiO_2 helps to improve the mechanical performance of mortars and concretes due to the filler effect of both additions and the pozzolanic effect of the last one (22). Therefore, the results reported in this paper suggest that the curing conditions play an important role with regard to the compressive strength.

Nano-SiO_2 performance has customarily been reported as increasing the compressive strength of mortars (7-9) and concretes (11-13) as a result of the pozzolanic and filler effect (22). The finer the SiO_2 in the mortar, the higher is the strength of the cement-based material (5). Moreover, the grain size distribution of the material (GSD) is also found to be of significant importance (5). In contrast, the results obtained in this paper are reversed. The incorporation of nano-SiO_2 and nano-Fe_2O_3 in the mortars leads to less compressive strength, as can be observed in Figure 3. This negative effect on the mechanical strength of mortars can be produced not only by insufficient nano-SiO_2 and nano-Fe_2O_3 dispersion during the mixing operation (7, 22), but also by an unsuitable curing method (in a cabinet at 95% relative humidity). On many occasions, those published studies that identified enhanced mechanical strength cured the mortars in full immersion (7, 9). Such a curing condition also leads to lower mortar compressive strengths than mortars cured at standard ones which are 30 MPa at two days and 61 MPa at 28 days (Table 1).

According to Sajedi and Razak (29), strength loss in Portland cement mortars depends on the cement fineness and regime of curing. They suggest

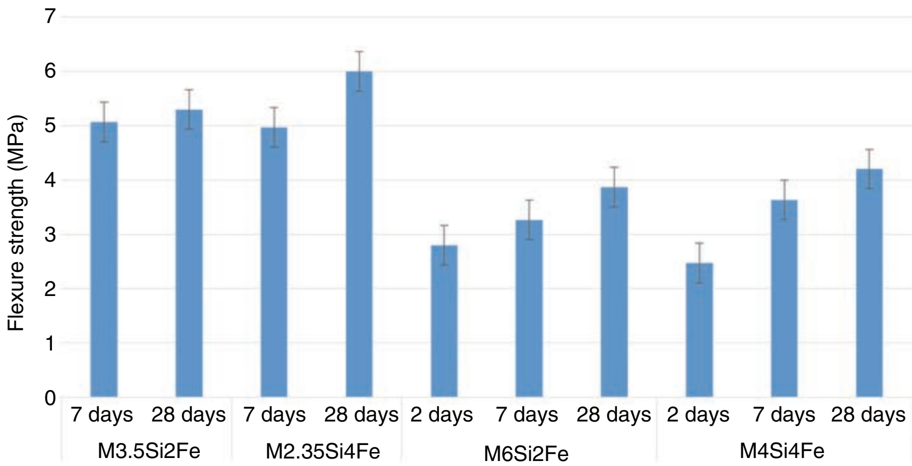

FIGURE 2. Flexure strength results and standard deviation (MPa).

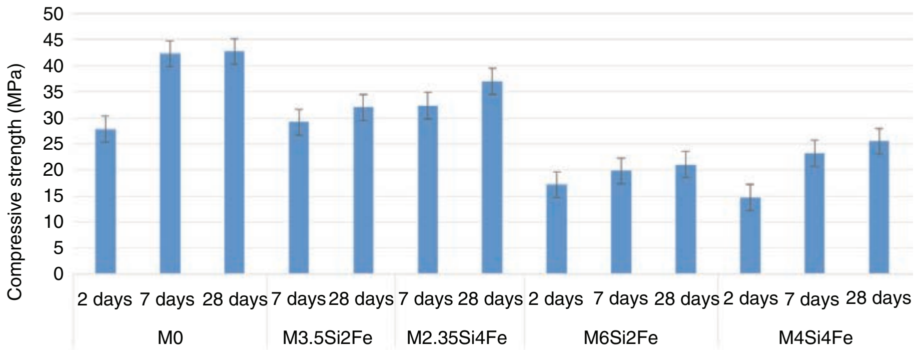

FIGURE 3. Compressive strength results and standard deviation (MPa).

that the main cause of mortar strength loss with the use of fine binders is due to phase separation, given that there is insufficient interlocking on the interfacial area. Another cause related with loss of strength involves the formed hydrates having no time to become arranged suitably. Lastly, the lack of internal water in the mortar could avoid proper hydration.

3.2. Mercury intrusion porosimetry

The earlier mentioned MIP was performed at 28 days and the results are shown in Figure 4. The main peak identified was the critical diameter for each mortar sample, as Table 5 shows.

Mortar M4Si4Fe had the highest critical diameter (1.054μm), followed by mortar M6Si2Fe (0.834μm). This value decreased sharply to 0.183μm for the mortar with 3.5% nano-SiO_2 (M3.5Si2Fe) and to 0.151μm for the mortar with 2.35% nano-SiO_2 (M2.35Si4Fe). Contrary to what was expected, the reference mortar presented the lowest critical diameter (0.063). The curves could be classified in three main groups: with about 8%, 6% or 0% of nano-oxides. The curves moved from the left to the right when nano-oxides were added, showing a pore-size increase. These results were in line with the compressive and flexural strength ones.

In agreement with the mechanical results, critical mean diameter pores determined by MIP could be ordered from the higher to lower size as follows:

M0 < M2.35Si4Fe < M3.5Si2Fe < M6Si2Fe < M4Si4Fe

Often nano-additions, as well as other additions, act by refilling the open spaces between the aggregates and cement paste. This improves the quality of the transition zone. They are located in the capillary pores and refine pore-size distribution (17). In particular, nano-SiO_2 combined with the $Ca(OH)_2$ produced in the calcium silicates hydration creates a secondary C-S-H gel at later ages, which is deposited in the capillary pores among other parts of the cement paste porous system (8).

Whereas Figure 5 plots the total porosity of the mortars at 28 days, Figure 6 shows the pore-size distribution (PSD). With regard to the total porosity, it may be observed that all the values obtained from mortars with nano-oxides showed high values from

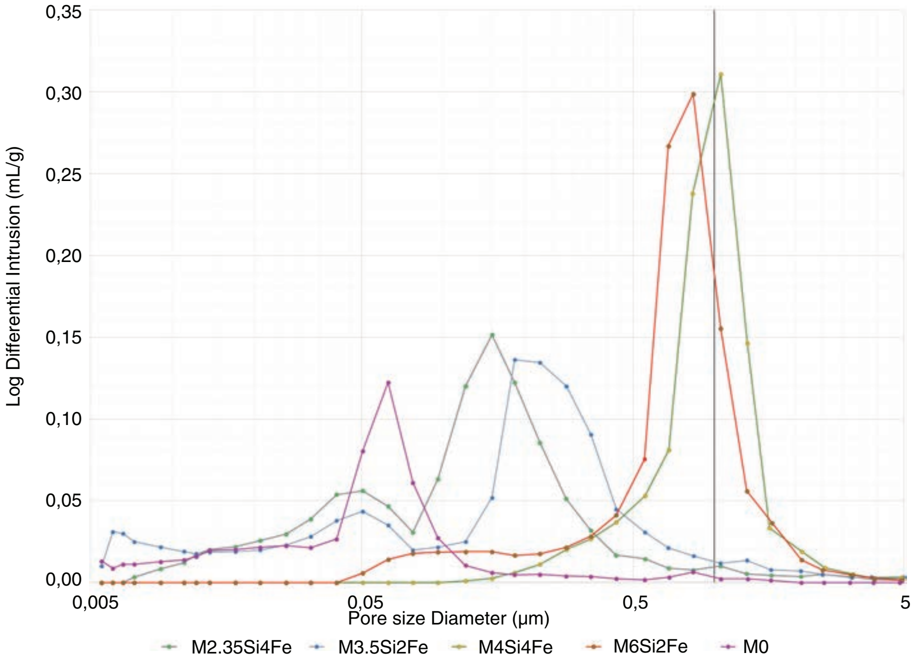

Figure 4. Differential mercury intrusion porosimetry (MIP) at 28 days.

Table 5 Critical diameter of the mortars at 28 days

Mix code	M0	M3.5Si2Fe	M2.35Si4Fe	M6Si2Fe	M4Si4Fe
Critical diameter (µm) at 28 days	0.063	0.183	0.151	0.834	1.054

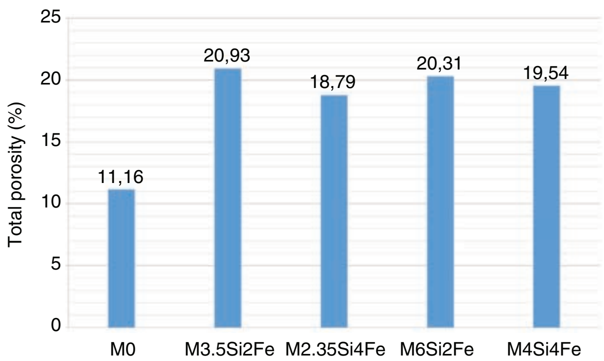

Figure 5. Total porosity (%) of the mortars at 28 days.

18.8% to 20.9%, double those of the total porosity of the reference mortar (M0). Thus, it is clear that nano-additions in a range of 4-8% of cement replacement in mortars, when mixed and cured following the procedure previously mentioned, produce an increase in total porosity of the mortars with regard to the reference one. This detrimental effect can be explained in two ways: i) the agglomeration effect of nano-oxides in mortar (7, 21, 22) was not fully addressed by using a commercial polycarboxylate-based superplasticizer admixture; ii) pozzolanic materials were highly sensitive to curing conditions, as they require a longer wet period with a continuous water supply (1). Therefore, 95% of relative humidity curing could be considered insufficient for mortars containing 4-8% of nano-oxides.

As a result, in the PSD analyses of mortars (Figure 6) the capillary-pore content increases with the nano-oxide amount which provides agreement with the flexural and compressive strength results.

In theory, nano-particles are uniformly dispersed in mortar and when hydration begins, hydrate products diffuse and cover nano-particles (13) which could restrict the growth of hexagonal $Ca(OH)_2$ crystals and promote cement hydration nucleation sites. The result is a more homogeneous and compact matrix (13). In this research, however, it was found that the more nano-SiO_2 there was in the mortar, the greater was the capillary-pore formation. Then, the reference mortar showed the lowest capillary porosity. Although such results agree with the compressive strength results, they differ from those provided in other published studies (7-16).

Other researchers (14) have observed that nano-silica (NS) added at ratios of 0.5% to 1.25% improved compressive strength of the mortars at all ages compared with the control specimens (the

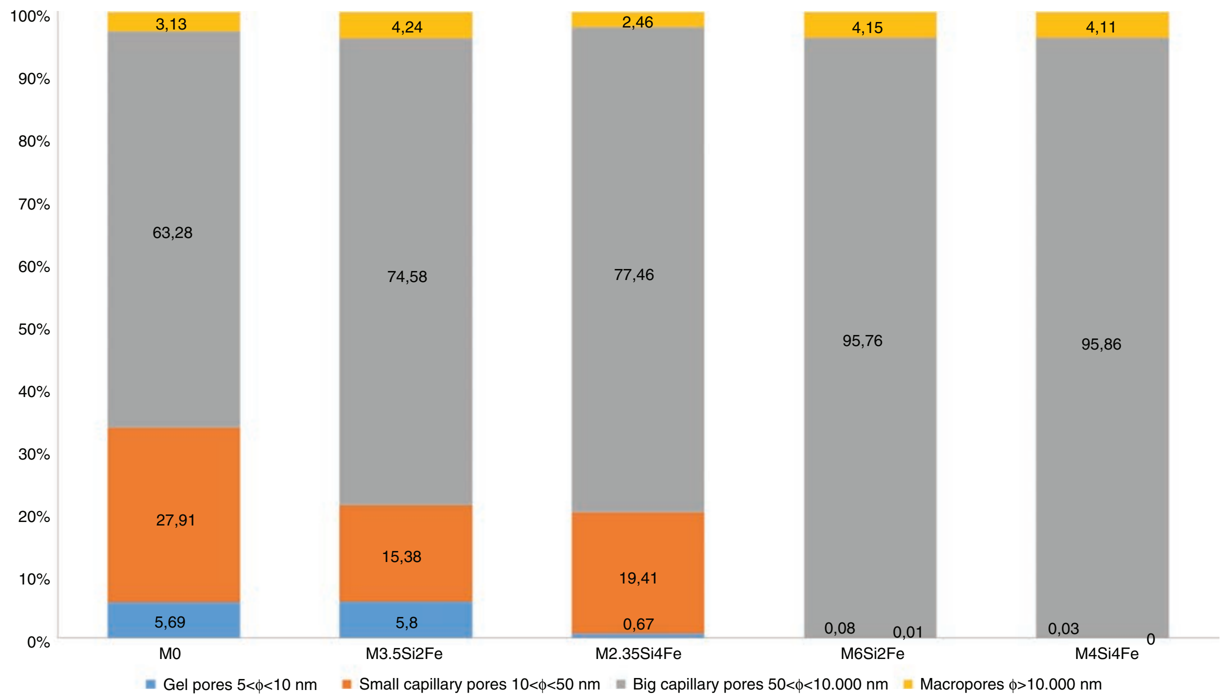

FIGURE 6. Pore-size distribution (PSD) of the mortars at 28 days.

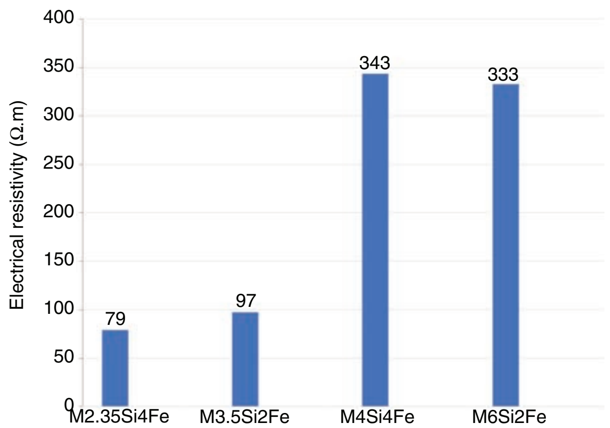

FIGURE 7. Electrical resistivity of the mortars.

rate of improvement varied between 5% and 15%). In specimens containing nano-silica powder at a rate of 2.5%, strength reduction appeared to vary between 43% and 60%. In addition, for nano-Fe_2O_3 it is observed that with the decrease in nano-Fe_2O_3 volume fraction (from 10% to 3%) the compressive strength increases at all ages (8).

3.3. Resistivity

Resistivity measurements have recently been used to assess the quality of cement-based materials (26). There is a clear relationship with the chloride diffusion coefficient (27) or the corrosion-rate measurements (28). Figure 7 shows two main groups with regard to the nano-oxide performance in the mortar.

Whereas the first group included M2.35Si4Fe and M3.5Si2Fe and exhibited electrical resistivity of around 100 Ω·m, the second one reached values below 350 Ω·m. Consequently, these last mortars will perform better in aggressive environments than the first ones (26, 27, 28). Therefore, the higher amount of nano-SiO_2 promoted the increase in durability. By comparing these values with those presented in Table 4, it could be argued that the first group of values corresponded to mortars with moderate chloride diffusivity, while the second one should have had very low chloride diffusivity.

Summarising, electrical resistivity measurements were recorded in order to obtain an indirect durability indicator of the mortars. In this case, as the amount of nano-oxides in the mortar increased, a greater degree of durability was found.

According to Andrade and D'Andrea (30), as resistivity is a property that depends on the concrete porous system and its degree of moisture, it is possible to find relations between diffusivity and resistivity. The authors have also suggested that resistivity could be used as a corrosion indicator.

4. CONCLUSION

The positive expected effect in compressive and flexural strength, in addition to durability, found when nano-SiO_2 or nano-Fe_2O_3 are added to

Portland cement mortars, can be reversed if the curing conditions and/or the nano-addition dispersing procedure are inefficient.

When the nano-Fe_2O_3 content is kept constant, the nano-SiO_2 increase leads to a compressive strength decrease for all the ages. In such a case, an increase of pores smaller than 50 nm will have also been observed.

ACKNOWLEDGEMENTS

The authors gratefully acknowledge the financial support provided by Ministry of Economy and Competitiveness of Spain by means of the Research Fund Project BIA 2016-78742-C2-2-R.

REFERENCES

1. Pavía, H.; Velosa, A.; Cachim, P.; Ferreira, V.M. (2016) Effect of pozzolans with different physical and chemical characteristics on concrete properties. *Mater. Construcc.* 66 [322], e083. https://doi.org/10.3989/mc.2016.01815
2. Fairbairn, E.M.R.; Americano, B.B.; Cordeiro, G.C.; Paula, T.P.; Toledo Filho, R.D.; Silvoso, M.M. (2010) Cement replacement by sugar cane bagasse ash: CO_2 emissions reduction and potential for carbon credits. *J. Environ. Manag.* 91 [9], 1864–1871. https://doi.org/10.1016/j.jenvman.2010.04.008
3. Argiz, C.; Menéndez, E.; Sanjuán, M.A. (2013) Effect of mixes made of coal bottom ash and fly ash on the mechanical strength and porosity of Portland cement. *Mater. Construcc.* 309, 49–64. https://doi.org/10.3989/mc.2013.03911
4. Roux, N.; Andrade, C.; Sanjuán, M. (1996) Experimental Study of Durability of Reactive Powder Concretes. *J. Mater. Civil Eng.* 8 [1], 1–6. https://doi.org/10.1061/(ASCE)0899-1561(1996)8:1(1)
5. Sanjuán, M.A.; Argiz, C.; Gálvez, J.C.; Moragues, A. (2015) Effect of silica fume fineness on the improvement of Portland cement strength performance. *Constr. Build. Mater.* 96, 55–64. https://doi.org/10.1016/j.conbuildmat.2015.07.092
6. Qing, Y.; Zenan, Z.; Deyu, K.; Rongshen, Ch. (2007) Influence of nano-SiO2 addition on properties of hardened cement paste as compared with silica fume. *Constr. Build. Mater.* 21(3), 539–545. https://doi.org/10.1016/j.conbuildmat.2005.09.001
7. Haruehansapong,S.; Pulngern, T.; Chucheepsakul, S. (2014) Effect of the particle size of nanosilica on the compressive strength and the optimum replacement content of cement mortar containing nano-SiO_2. *Constr. Build. Mater.* 50, 471–477. https://doi.org/10.1016/j.conbuildmat.2013.10.002
8. Li, H.; Xiao, H.; Yuan, J.; Ou, J. (2004) Microstructure of cement mortar with nano-particles. *Compos Part B Eng.* 35 [2], 185–189. https://doi.org/10.1016/S1359-8368(03)00052-0
9. Jo, B.W.; Kim, C.H.; Tae, G.H. (2007) Characteristics of cement mortar with nano-SiO_2 particles. *Construct. Build. Mater.* 21, 1351–1355. https://doi.org/10.1016/j.conbuildmat.2005.12.020
10. Lin, K.L.; Chang, W.C.; Lin, D.F.; Luo, H.L.; Tsai, M.C. (2008) Effects of nano-SiO_2 and different ash particle sizes on sludge ash-cement mortar. *J. Environ. Manage.* 88 [4], 708–714. https://doi.org/10.1016/j.jenvman.2007.03.036
11. Ji, T. (2005) Preliminary study on the water permeability and microstructure of concrete incorporating nano-SiO_2. *Cem. Concr. Res.* 35 [10], 1943–1947. https://doi.org/10.1016/j.cemconres.2005.07.004
12. Nazari, A.; Riahi, S. (2011) Splitting tensile strength of concrete using ground granulated blast furnace slag and SiO_2 nano-particles as binder. *Energ. Buildings* 43 [4], 864–872. https://doi.org/10.1016/j.enbuild.2010.12.006
13. Jalal, M.; Mansouri, E.; Sharifipour, M.; Pouladkhan, A.R. (2012) Mechanical, rheological, durability and microstructural properties of high performance self-compacting concrete containing SiO_2 micro and nanoparticles. *Mater. Design* 34, 389–400. https://doi.org/10.1016/j.matdes.2011.08.037
14. Oltulu, M.; Sahin, R. S. (2011) Single and combined effects of nano-SiO_2, nano-Al_2O_3 and nano-Fe_2O_3 powders on compressive strength and capillary permeability of cement mortar containing silica fume. *Mater. Sci. Eng. A* 528 [22–23], 7012–7019. https://doi.org/10.1016/j.msea.2011.05.054
15. Mohseni, E.; Miyandehi, B.M.; Yang, J.; Yazdi, M.A. (2015) Single and combined effects of nano-SiO_2, nano-Al_2O_3 and nano-TiO_2 on the mechanical, rheological and durability properties of self-compacting mortar containing fly ash. *Constr. Build. Mater.* 84, 331–340. https://doi.org/10.1016/j.conbuildmat.2015.03.006
16. Horszczaruk, E.; Mijowska, E.; Cendrowski, K.; Mijowska, S.; Sikora, P. (2014) Effect of incorporation route on dispersion of mesoporous silica nanospheres in cement mortar. *Constr. Build. Mater.* 66, 418–421. https://doi.org/10.1016/j.conbuildmat.2014.05.061
17. Kontoleontos, F.; Tsakiridis, P.E.; Marinos, A.; Kaoidas, V.; Katsioti, M. (2012) Influence of colloidal nanosilica on ultrafine cement hydration: Physicolchemical and microstructural characterization. *Constr. Build. Mater.* 35, 347–360. https://doi.org/10.1016/j.conbuildmat.2012.04.022
18. Sáez del Bosque, I.F.; Martínez-Ramírez; S.; Blanco-Varela, M.T. (2015) Calorimetric study of the early stages of the nanosilica - tricalcium silicate hydration. Effect of temperature. *Mater. Construcc.* 65 [320], e070. https://doi.org/10.3989/mc.2015.06814
19. Thomas, J.J.; Jennings, H.M.; Chen, J.J. (2009) Influence of Nucleation Seeding on the Hydration Mechanisms of Tricalcium Silicate and Cement. *J. Phys. Chem. C* 113 [11], 4327–4334. https://doi.org/10.1021/jp809811w
20. Land, G.; Stephan, D. (2012) The influence of nano-silica on the hydration of ordinary Portland cement. *J. Mater. Sci.* 47 [2], 1011–1017. https://doi.org/10.1007/s10853-011-5881-1
21. Tashima, M.M.; Soriano, L.; Monzó, J.; Borrachero, M.V.; Akasaki, J.L.; Payá, J. (2014) New method to assess the pozzolanic reactivity of mineral admixtures by means of pH and electrical conductivity measurements in lime:pozzolan suspensions. *Mater. Construcc.* 64 [316], e032 https://doi.org/10.3989/mc.2014.00914
22. Kong, D.; Du, X.; Wei, X.; Zhang, H.; Yang, Y.; Shah, S. P. (2012) Influence of nano-silica agglomeration on microstructure and properties of the hardened cement-based materials. *Constr. Build. Mater.* 37, 707–715. https://doi.org/10.1016/j.conbuildmat.2012.08.006
23. EN 196–1 (2016) Methods of testing cement - Part 1: Determination of strength. European Committee for Standardization (CEN), Brussels.
24. EN 934–2 (2009) Admixtures for concrete, mortar and grout - Part 2: Concrete admixtures - Definitions, requirements, conformity, marking and labelling. European Committee for Standardization (CEN), Brussels.
25. ASTM C1202 (2012) Standard Test Method for Electrical Indication of Concrete's Ability to Resist Chloride Ion Penetration. Book of Standards Volume: 04.02. ASTM International, West Conshohocken, PA, 19428–2959 USA.
26. UNE 83988–1 (2008) Concrete durability. Test methods. Determination of the electrical resistivity. Part 1: Direct test (reference method). AENOR, Madrid.
27. Andrade, C. (1993) Calculation of chloride diffusion coefficients in concrete from ionic migration measurements. *Cem. Concr. Res.* 23 [3], 724–742. https://doi.org/10.1016/0008-8846(93)90023-3
28. Sanjuán M.A. (2000) Overview on electrochemical parameters to assess the corrosion state of steel reinforcement in calcium aluminate cement mortar and concrete. *J. Mater. Sci.* 35 [1], 105–108. https://doi.org/10.1023/A:1004748801193

29. Sajedi, F.; Razak, H.A. (2011) Effects of curing regimes and cement fineness on the compressive strength of ordinary Portland cement mortars. *Constr. Build. Mater.* 25, 2036–2045. https://doi.org/10.1016/j.conbuildmat.2010.11.043

30. Andrade, C.; D'Andrea, R. (2010) Electrical resistivity as microstructural parameter for the modelling of service life of reinforced concrete structures. 2nd International Symposium on Service Life Design for Infrastructure, 4–6 October 2010, Delft, The Netherlands. 379–388.